ACS OMEGA

http://pubs.acs.org/journal/acsodf

Article

Thermodynamic Analysis on *In Situ* Underground Pyrolysis of Tar-Rich Coal: Secondary Reactions

Deliang Fu,[§] Zunyi Yu,[§] Kun Gao, Zhonghui Duan, Zhendong Wang, Wei Guo, Panxi Yang, Jie Zhang, Bolun Yang, Fu Yang, and Zhiqiang Wu*

Cite This: *ACS Omega* 2023, 8, 12805−12819

Read Online

ACCESS | Metrics & More | Article Recommendations | Supporting Information

ABSTRACT: To develop the *in situ* underground pyrolysis process of tar-rich coal more scientifically, the effect of temperature and pressure on the distribution of pyrolysis products should be clarified. This paper selected the typical components in five distillates of light tar, phenol tar, naphthalene tar, washing tar, and anthracene tar as the main reaction products. 32 typical secondary reactions were constructed. Based on the thermodynamic analysis strategy, the variation of the Gibbs free energy and equilibrium constant of secondary reactions was investigated. The results showed that pressure mainly affected the reaction characteristics of molecule-increasing reactions. The Gibbs free energy value of the molecule-increasing reactions increased with increasing pressure. The trend that the reaction could proceed spontaneously gradually weakened. The initial temperature of some reactions that could proceed spontaneously would need to increase by dozens or even hundreds of degrees. Due to the influence of formation pressure, the generation of related components of light tar, naphthalene tar, washing tar, and anthracene tar would be inhibited to varying degrees in the *in situ* underground pyrolysis process. The secondary reactions related to phenol tar were equimolecular reactions, which were almost unaffected by stratal pressure. Axial pressure and confining pressure of different coal seam depths should be considered in the process of *in situ* underground pyrolysis.

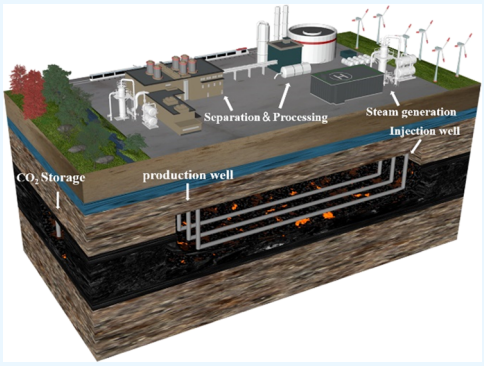

1. INTRODUCTION

Global coal resources are abundant, but the excessive utilization in the early stage has caused a series of environmental problems, such as air pollution and the greenhouse effect, which has seriously hindered the sustainable development of the world economy. Therefore, improving its utilization significantly alleviates the world's environmental crisis.[1,2] Based on the tar yield, coal could be roughly divided into high-tar coal (Tar, d > 12%), tar-rich coal (Tar, d = 7−12%), and tar-containing coal (Tar, d < 7%). Tar-rich coal generally includes high-tar coal and tar-rich coal.[3] The most typical feature of tar-rich coal is its many hydrogen-rich structures, and the hydrogen-rich structure mainly refers to the weak bond structure attached to the edge of a condensed aromatic nucleus or the branched chain and side chain of an aromatic nucleus and the bridge bond between the aromatic nucleus. They are mainly composed of methyl, methylene, methine, and quaternary carbon. Hydrogen-rich structures could be decomposed and volatilized to produce tar and gas during pyrolysis.[4−7]

Currently, the utilization of tar-rich coal is still dominated by conventional pyrolysis. Conventional pyrolysis refers to the technology of mining, washing, and transporting coal to the ground, followed by pyrolysis treatment and subsequent processing, which has practical problems such as high energy demand, low utilization rate, and large environmental pollution. There is still a risk of stratal collapse in long-term mining.[8,9]

The *in situ* underground pyrolysis of tar-rich coal means that the coal is no longer mined by traditional methods but directly underground through fracturing, injecting proppant, and transferring heat to the coal seam through heat-transfer mediums. Tar and gas are transported to the ground through mining wells for subsequent processing.[10−14] This technology realizes quality improvement and utilization of coal from the source and has distinctive characteristics of environmental friendliness, excellent tar quality, and high production safety. Certainly, there are still some challenges in this technology. For example, efficient heat transfer is still being explored, and it is difficult to extract pyrolysis products. But overall, *in situ* underground pyrolysis is a very promising technology for tar-rich coal utilization.

Received: December 18, 2022
Accepted: March 21, 2023
Published: March 28, 2023

https://doi.org/10.1021/acsomega.2c08033
ACS Omega 2023, 8, 12805−12819

Generally speaking, the reaction systems in secondary reactions between *in situ* underground pyrolysis and conventional pyrolysis are similar. The main difference is the reaction conditions. Due to the *in situ* underground pyrolysis being affected by axial pressure and confining pressure from strata, it is carried out under high pressure, the liberation of volatile is difficult, the residence time between coal seams is longer, and the secondary reaction is more thorough. Due to the coal not being mined, the size of the pyrolysis coal sample is large. Moreover, before the start of *in situ* underground pyrolysis, the coal seam should be cracked, and proppant should be injected to prevent collapse formation. With the continuous liberation of volatiles during pyrolysis, many pores would be generated inside the coal sample. In comparison, conventional pyrolysis is usually carried out under atmospheric pressure, and coal samples are usually pulverized coal particles. Because conventional pyrolysis is not affected by pressure, the liberation of volatiles is easier, so the secondary reaction proceeds to a lesser extent. The temperature of *in situ* underground pyrolysis is generally lower than 600 °C, making the probability of pollutants (such as sulfide) decomposing and being released from the coal seam less likely. In addition, the semi-coke obtained has developed a pore structure, which could be used as the perfect adsorption site for pollutants and CO_2. The semi-coke remains underground, avoiding hollow formation and effectively preventing collapse formation.

Zhang et al.[8] summarized and analyzed the heating mode, affecting factors, economic cost, technical challenges, and ecological problems of *in situ* underground pyrolysis of tar-rich coal. Wang et al.[15] studied the pressurized pyrolysis of Taiheiyo coal at the final temperature of 800 °C in a tubular furnace. The results showed that when the pressure increased from 0.3 to 1.0 MPa and 3.0 MPa, the tar yield decreased from 16 to 13 and 9%, respectively. Chareonpanich et al.[16] showed that the tar yield of Liddell coal decreased from 22 to 17 and 14%, respectively, when the pyrolysis pressure increased from 0.1 to 2.0 and 5.0 MPa at 600 °C. Zu et al.[17] studied the pressurized pyrolysis characteristics of Buliangou coal at 700 °C. They discovered that when the pyrolysis pressure increased from 0.1 to 1.5 and 3.5 MPa, the tar yield decreased from 4.63 to 3.64 and 2.88%, respectively. Liang et al.[18] studied the pressurized pyrolysis of Xiaolongtan coal and Yima coal in N_2 and H_2 atmospheres, respectively. The findings indicated that in a N_2 atmosphere, the tar yield gradually decreased with increasing pressure. In contrast, in a H_2 atmosphere, the tar yield first increased and then decreased as the pressure increased. The contents of BTX (benzene, toluene, xylene) and PCX (phenol, cresol, xylenol) in tar gradually increased with increasing pressure, and the content of aliphatic compounds gradually decreased with increasing pressure. Liu et al.[19] studied the pyrolysis characteristics of Tianzhu coal in N_2 and H_2 atmospheres, and the results showed that the change tendency in tar yield with pressure was consistent with that by Liang et al.[18] Also, Liu et al.[19] found that the contents of BTX and PCX in tar showed an increasing trend with increasing pressure, and the aliphatic compound content gradually decreased with increasing pressure. *In situ* underground pyrolysis technology enables the utilization of deeply buried coal. High-quality tar and gas could be obtained by optimizing pyrolysis conditions, which is of great significance in alleviating the pressure of oil and gas resources and realizing the green and efficient utilization of coal.[20]

The secondary reaction of coal pyrolysis refers to the process in which the products of the primary reaction separate from the coal seam. Due to external factors such as temperature and pressure, the free radical fragments in the volatile are decomposed and polymerized, thus affecting the yield and distribution of the final product.[21] The degree of secondary reaction would directly affect the yield and quality of tar, so the secondary reaction plays an important role in coal pyrolysis.[20,22,23] The main factors of secondary reaction are temperature, pressure, residence time, and pyrolysis atmosphere. Higher temperature and pressure and longer residence time could intensify the secondary reaction, thus affecting the tar obtained from pyrolysis.[24] Katheklakis et al.[25] studied the effect of the residence time of volatiles on the molecular weight of tar in a fluidized bed reactor. The results showed that a higher pyrolysis temperature and longer residence time would significantly reduce the molecular weight of tar. Hayashi et al.[26] studied the effect of temperature on the molecular structure of tar in a fluidized bed reactor, and the findings indicated that the H/C atomic ratio in tar decreased with increasing temperature. Ariunaa et al.[27] showed that the tar yield was higher in the H_2 atmosphere than in the N_2 atmosphere under the same conditions. Currently, the study on coal pyrolysis mainly focuses on the product yield and the improvement of specific component content. Still, there are few studies on the source's specific chemical reactions involved in the pyrolysis process. Temperature and pressure have an important effect on the secondary reaction, which could often be reflected by changing the thermodynamic state function of the reaction process. Therefore, according to the reaction conditions of *in situ* underground pyrolysis, it is of great significance to explore the effect of pressure and temperature on thermodynamic characters for the regulation of the secondary reaction process. Gibbs free energy is a thermodynamic parameter introduced in chemical thermodynamics to determine the direction of the reaction process. The Gibbs free energy of the reaction has a direct relationship with temperature and pressure. Therefore, by calculating and analyzing the change trend of Gibbs free energy with temperature and pressure, the direction or limit of secondary reaction could be indirectly clarified when the temperature or pressure changes. The equilibrium constant is the thermodynamic parameter used to indicate the extent to which the chemical reaction proceeds. Under the same conditions, a large equilibrium constant means that the reaction is carried out to a greater extent. Both temperature and pressure have an important influence on the equilibrium constant.

In this paper, the tar was cut according to the boiling point of distillation, and the main components of each distillate were analyzed. Some typical secondary reactions were constructed, and the thermodynamic analysis of each reaction was carried out. The variation of Gibbs free energy and equilibrium constant of the reactions in the temperature and pressure ranges of 300−900 °C and 0.1−10 MPa, respectively, were explored to provide theoretical reference for the research and development of *in situ* underground pyrolysis technology of tar-rich coal.

2. MODELS AND METHODS

2.1. Construction of the Typical Secondary Reactions.

As shown in Table 2, most of the 32 typical secondary reactions listed are based on the published literature. For a few secondary reactions not found in the literature, based on the

https://doi.org/10.1021/acsomega.2c08033
ACS Omega 2023, 8, 12805−12819

results of distillate cutting in Table 1, the main components in tar as the main reaction products, combined with the type and yield of other gaseous products obtained from the pyrolysis experiments, the secondary reactions were constructed (Table 2).

Table 1. Tar Distillation Fractions and Typical Components[28]

distillate	boiling point range (°C)	main components
light tar	<170	benzene, toluene, xylene, octane, etc.
phenol tar	170−210	phenol, cresol, dimethyl phenol, etc.
naphthalene tar	210−230	naphthalene, *n*-dodecane, etc.
washing tar	230−300	fluorene, acenaphthene, methylnaphthalene, dimethylnaphthalene, etc.
anthracene tar	300−360	anthracene, phenanthrene, carbazole, etc.
asphalt	>360	aromatic compounds with more than three rings

2.2. Analytical Method for Thermodynamic Characteristics of Secondary Reactions. Based on the actual reaction conditions of *in situ* underground pyrolysis of tar-rich coal, the thermodynamic parameters of each compound at 300−900 °C and 0.1−10 MPa were obtained from the physical property database. The Gibbs free energy, enthalpy change, and equilibrium constant of each typical secondary reaction were calculated, and the thermodynamic analysis of each secondary reaction was briefly carried out. The detailed values of Gibbs free energy and equilibrium constant are provided in the Supporting Information.

$$\Delta_r G_m^\theta = \Delta_r H_m^\theta - T\Delta_r S_m^\theta \quad (1)$$

Table 2. Secondary Reactions in the *In Situ* Pyrolysis of Tar-Rich Coal[21,23,24,29−41]

components	reaction type	reaction equation	literature
benzene	equimolecular	$C_6H_3(CH_3)_2OH + 3H_2 = C_6H_6 + H_2O + 2CH_4$ (R1)	40
benzene	equimolecular	$C_6H_4CH_3OH + 2H_2 = C_6H_6 + CH_4 + H_2O$ (R2)	37
benzene	equimolecular	$C_6H_5OH + H_2 = C_6H_6 + H_2O$ (R3)	21
benzene	equimolecular	$C_6H_4(CH_3)_2 + 2H_2 = C_6H_6 + 2CH_4$ (R4)	construction
benzene	equimolecular	$C_6H_5CH_3 + H_2 = C_6H_6 + CH_4$ (R5)	24
benzene	molecule-increasing	$C_6H_{12} = C_6H_6 + 3H_2$ (R6)	21
benzene	molecule-increasing	$C_4H_6 + C_2H_4 = C_6H_6 + 2H_2$ (R7)	32
toluene	equimolecular	$C_6H_3(CH_3)_2OH + 2H_2 = C_6H_5CH_3 + CH_4 + H_2O$ (R8)	41
toluene	equimolecular	$C_6H_4CH_3OH + H_2 = C_6H_5CH_3 + H_2O$ (R9)	40
toluene	equimolecular	$C_6H_4(CH_3)_2 + H_2 = C_6H_5CH_3 + CH_4$ (R10)	24
toluene	molecule-increasing	$C_7H_{16} = C_6H_5CH_3 + 4H_2$ (R11)	construction
toluene	molecule-increasing	$C_6H_{11}CH_3 = C_6H_5CH_3 + 3H_2$ (R12)	41
toluene	molecule-increasing	$C_4H_6 + C_3H_6 = C_6H_5CH_3 + 2H_2$ (R13)	41
xylene	equimolecular	$C_6H_3(CH_3)_2OH + H_2 = C_6H_4(CH_3)_2 + H_2O$ (R14)	40
octane	molecule-increasing	$C_{14}H_{30} = C_8H_{18} + C_6H_{12}$(ethylene) (R15)	41
octane	molecule-increasing	$C_{14}H_{30} = C_8H_{18} + C_6H_{12}$(cyclohexane) (R16)	41
octane	molecule-increasing	$C_{14}H_{30} = C_8H_{18} + C_6H_6 + 3H_2$ (R17)	41
phenol	equimolecular	$C_6H_4CH_3OH + H_2 = C_6H_5OH + CH_4$ (R18)	40
cresol	equimolecular	$C_6H_3(CH_3)_2OH + H_2 = C_6H_4CH_3OH + CH_4$ (R19)	40
naphthalene	molecule-increasing	$2C_6H_4CH_3OH = C_{10}H_8 + 2H_2O + CH_4 + 3C$ (R20)	construction
naphthalene	molecule-increasing	$2C_6H_5OH = C_{10}H_8 + 2H_2O + 2C$ (R21)	41
naphthalene	molecule-increasing	$2C_6H_5OH = C_{10}H_8 + 2CO + 2H_2$ (R22)	32
naphthalene	molecule-increasing	$C_4H_6 + C_6H_6 = C_{10}H_8 + 2H_2$ (R23)	24
naphthalene	molecule-increasing	$2C_6H_5CH_3 = C_{10}H_8 + 2CH_4 + 2C$ (R24)	41
naphthalene	equimolecular	$2C_6H_6 = C_{10}H_8 + CH_4 + C$ (R25)	construction
n-dodecane	molecule-increasing	$C_{14}H_{30} = C_{12}H_{26} + CH_4 + C$ (R26)	24
methylnaphthalene	molecule-increasing	$C_6H_5CH_3 + C_6H_4CH_3OH = C_{11}H_{10} + CH_4 + H_2O + 2C$ (R27)	construction
dimethylnaphthalene	equimolecular	$2C_6H_5CH_3 = C_{12}H_{12} + CH_4 + C$ (R28)	construction
anthracene	molecule-increasing	$2C_6H_4CH_3OH = C_{14}H_{10} + 2H_2O + H_2$ (R29)	construction
anthracene	molecule-increasing	$C_4H_6 + C_{10}H_8 = C_{14}H_{10} + 2H_2$ (R30)	21
anthracene	molecule-increasing	$2C_6H_5CH_3 = C_{14}H_{10} + 3H_2$ (R31)	41
anthracene	molecule-increasing	$C_6H_6 + C_6H_4(CH_3)_2 = C_{14}H_{10} + 3H_2$ (R32)	33

https://doi.org/10.1021/acsomega.2c08033
ACS Omega 2023, 8, 12805−12819

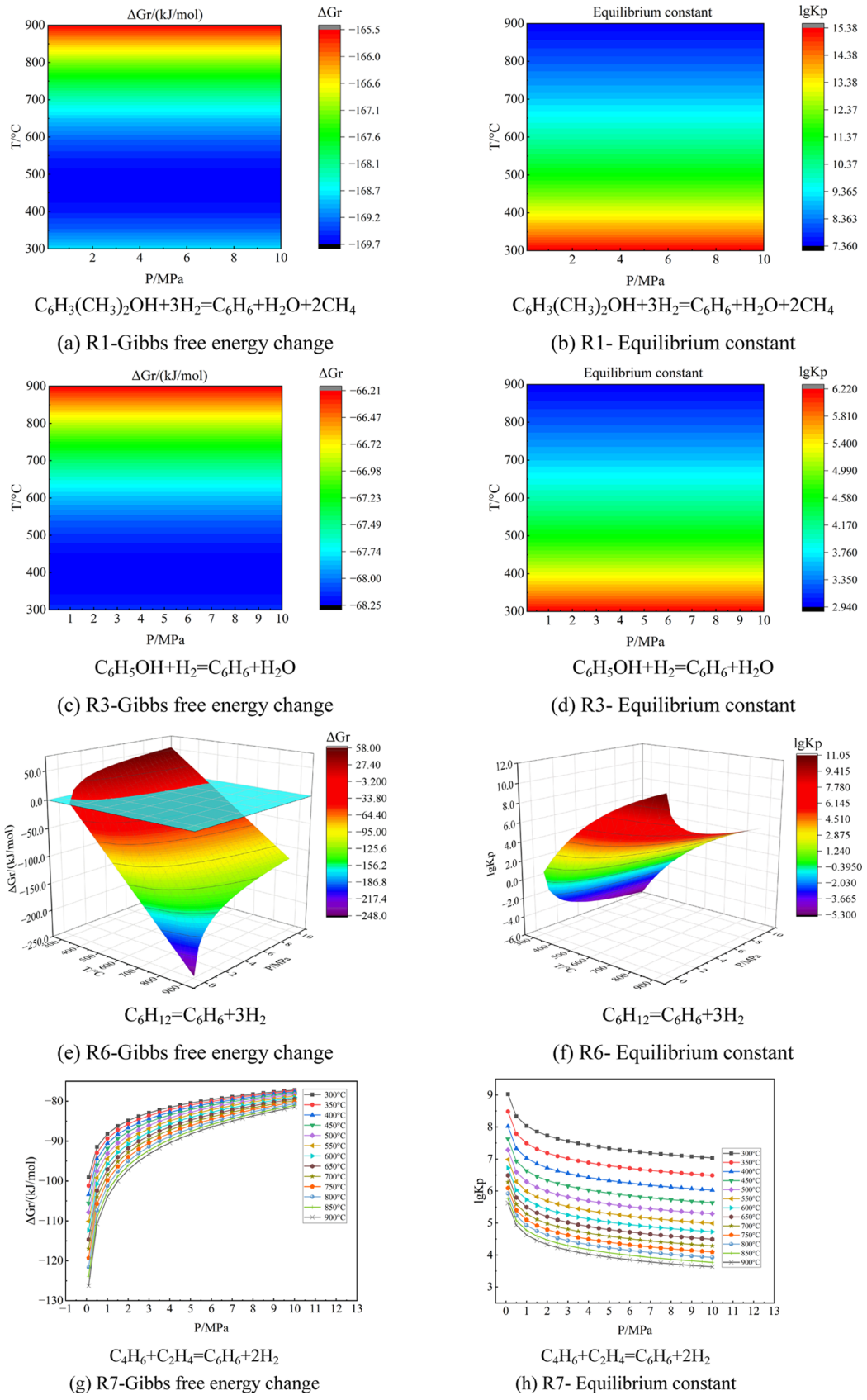

Figure 1. Effects of temperature and pressure on the Gibbs free energy and equilibrium constant of R1 (a, b), R3 (c, d), R6 (e, f), and R7 (g, h).

$$K_p = \exp(\Delta_r G_m^\theta / RT) \quad (2)$$

where $\Delta_r G_m^\theta$ is the standard Gibbs free energy change of formation, kJ mol^{-1}. $\Delta_r H_m^\theta$ is the standard enthalpy change of formation, kJ mol^{-1}. $\Delta_r S_m^\theta$ is the standard entropy change, J

https://doi.org/10.1021/acsomega.2c08033
ACS Omega 2023, 8, 12805−12819

(mol K)$^{-1}$. K_p is the equilibrium constant. R is the gas molar constant, 8.314 J (mol K)$^{-1}$. T is the temperature, °C.

2.2.1. Effect of Temperature on the Thermodynamic Parameters of Secondary Reactions. According to Kirchhoff 's law,[42] the relationship between enthalpy and temperature is shown in eq 3

$$\Delta_r H_m(T_2) = \Delta_r H_m(T_1) + \int_{T_1}^{T_2} \Delta C_p dT \tag{3}$$

where $\Delta_r H_m$ is the reaction enthalpy change, kJ mol^{-1}, and C_P is the heat capacity, J (kg K)$^{-1}$.

The relationship between heat capacity and temperature is as follows[43−45]

$$C_p = A + B\cdot 10^{-3}\cdot T + C\cdot 10^{5}\cdot T^{-2} + D\cdot 10^{-6}\cdot T^{2} \tag{4}$$

In the formula, A, B, C, and D are constants obtained by regression of experimental data, which could be searched according to experimental conditions. For the same substance under the same reaction conditions, the values of A, B, C, and D in eqs 4, 6, and 8 are the same.

The relationship between the standard formation enthalpies of coal and temperature is shown in eq 5

$$H_{coal} = \frac{R}{M_a}\left[380 g_0\left(\frac{380}{T}\right) + 3600 g_0\left(\frac{3600}{T}\right)\right] \tag{5}$$

In the formula, $g_0(x) = \frac{1}{\exp(x)-1}$, M_a is the average molecular weight of coal, $M_a = \sum_{i=1}^{5} x_i M_{ai}$, and R is the molar gas constant, 8.314 J (mol K)$^{-1}$.

Substituting eqs 4 and 5 into eq 3, the relationship between the enthalpy change and temperature could be obtained as

$$\begin{aligned}\Delta_r H_m T = {} & \Delta_r H_m(T_0) + AT + B\cdot 10^{-3}\frac{T^2}{2} - \frac{C\cdot 10^{5}}{T} \\ & + D\cdot 10^{-6}\frac{T^3}{3} - \frac{R}{M_a}\left[380 g_0\left(\frac{380}{T}\right)\right. \\ & \left. + 3600 g_0\left(\frac{3600}{T}\right)\right]\end{aligned} \tag{6}$$

Equation 7 could be obtained from the Gibbs−Helmholtz formula[42]

$$\frac{\partial\left(\frac{\Delta_r G_m}{T}\right)}{\partial T} = \frac{-\Delta_r H_m}{T^2} \tag{7}$$

Substituting eq 6 into eq 7, we could obtain the variation of Gibbs free energy with temperature for the secondary reactions under constant pressure

$$\begin{aligned}\Delta_r G_m(T) = {} & -AT\ln T - \frac{B\cdot 10^{-3}}{2}T^2 - \frac{C\cdot 10^{-5}}{2\cdot T} + \frac{D\cdot 10^{-6}}{6} \\ & \cdot T^3 + \frac{R}{M_a}\cdot T\cdot\left[\frac{380}{T} - \ln\left(e^{380/T} - 1\right)\right] \\ & + \frac{R}{M_a}\cdot T\cdot\left[\frac{3600}{T} - \ln\left(e^{3600/T} - 1\right)\right] \\ & + \Delta_r H_m(T_0) + IT\end{aligned} \tag{8}$$

2.2.2. Effect of Pressure on the Thermodynamic Parameters of Secondary Reactions. According to Maxwell's equation,[42] the variation of Gibbs free energy of secondary reactions with temperature and pressure is shown in eq 9

$$dG = -SdT + Vdp \tag{9}$$

Suppose the temperature is constant, $dG = Vdp = nRT\frac{dp}{p}$. The relationship between Gibbs free energy and pressure of ideal gas at a constant temperature is shown in eq 10

$$\Delta_r G_m(T) = \Delta_r G_m^{\theta}(T) + nRT\ln\frac{p}{p^{\theta}} \tag{10}$$

Suppose the temperature is constant, the Gibbs free energy of the secondary reaction varies with pressure as follows

$$\Delta_r G_m(T) = \Delta_r G_m^{\theta}(T) + nRT\Pi\ln\left(\varphi_i\frac{p_i}{p^{\theta}}\right)^{v_i} \tag{11}$$

$$K_p = \exp\left[-\frac{\Delta_r G_m(T)}{RT}\right] \tag{12}$$

Based on the above equations, the values of Gibbs free energy change and equilibrium constant of each typical secondary reaction could be obtained in the range of 0.1−10 MPa and 300−900 °C. The relationship figures of Gibbs free energy change and equilibrium constant with temperature and pressure could be drawn, respectively.

3. RESULTS AND DISCUSSION

3.1. Thermodynamic Analysis of the Secondary Reaction to Generate Light Tar. *3.1.1. Secondary Reaction with Benzene as the Main Product.* R1−R7 are secondary reactions with benzene as the main product. Figure 1 shows the changes in the Gibbs free energy and equilibrium constant of R1, R3, R6, and R7 with temperature and pressure. Relevant figures for R2, R4, and R5 are provided in the Supporting Information. According to the relationship between the Gibbs free energy and temperature and pressure, the Gibbs free energy values of R1, R3, R4, R5, and R7 were less than 0 in the whole temperature and pressure range. The reactions could be carried out spontaneously. Under the same conditions, the Gibbs free energy value of R7 gradually increased with increasing pressure, and the trend that the reaction could proceed spontaneously gradually weakened. Only when the temperature was below 520 °C, the Gibbs free energy value of R2 was less than 0, and the reaction could proceed spontaneously. At the atmospheric pressure, the Gibbs free energy value of R6 was less than 0 in the whole temperature range. The temperature nodes with the Gibbs free energy value were equal to 0 and gradually increased with increasing pressure. When the pressure was high, R6 required a higher temperature to proceed spontaneously.

According to the relationship between equilibrium constant and temperature and pressure, the equilibrium constants of R1, R2, R3, R4, R5, and R7 gradually decreased with increasing temperature, so they were exothermic reactions. Similarly, R6 was an endothermic reaction. R1−R5 were equimolecular reactions, and R6 and R7 were molecule-increasing reactions. Macroscopically, the increases in temperature and pressure were not conducive to the forward progress of secondary reactions to generate benzene. Still, the results were inconsistent with those reported in the previous literature. They have shown that in a reducing atmosphere, the benzene content in the tar obtained from pyrolysis had an increasing

https://doi.org/10.1021/acsomega.2c08033
ACS Omega 2023, 8, 12805−12819

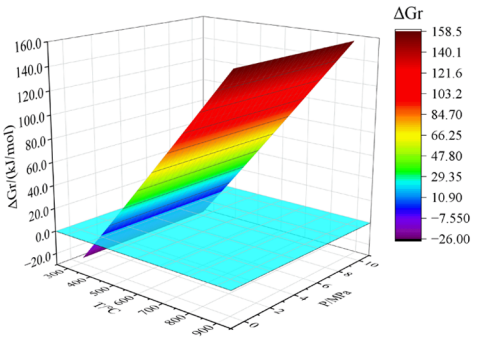

$C_6H_4CH_3OH+H_2=C_6H_5CH_3+H_2O$

(a) R9-Gibbs free energy change

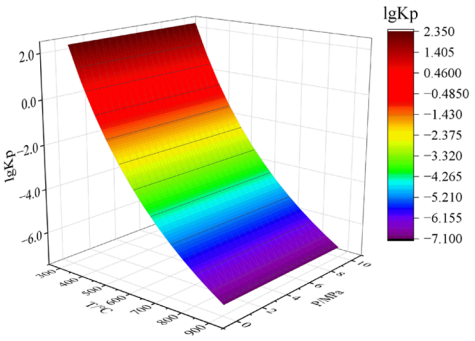

$C_6H_4CH_3OH+H_2=C_6H_5CH_3+H_2O$

(b) R9- Equilibrium constant

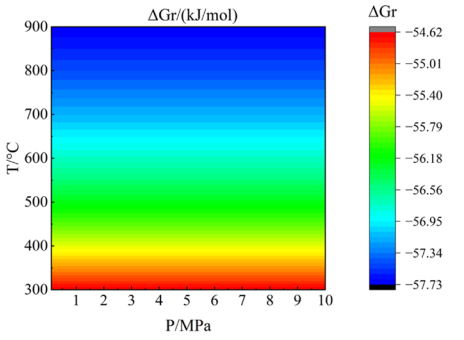

$C_6H_4(CH_3)_2+H_2=C_6H_5CH_3+CH_4$

(c) R10-Gibbs free energy change

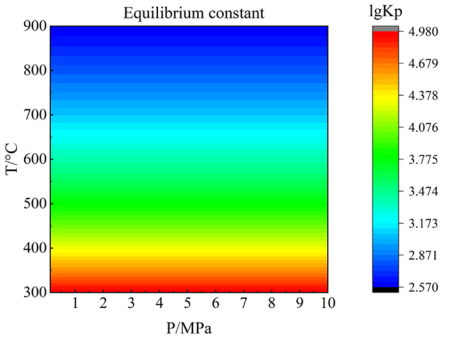

$C_6H_4(CH_3)_2+H_2=C_6H_5CH_3+CH_4$

(d) R10- Equilibrium constant

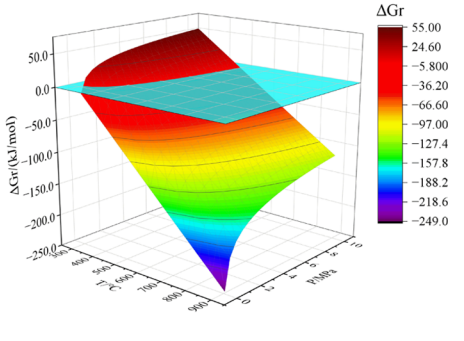

$C_6H_{11}CH_3=C_6H_5CH_3+3H_2$

(e) R12-Gibbs free energy change

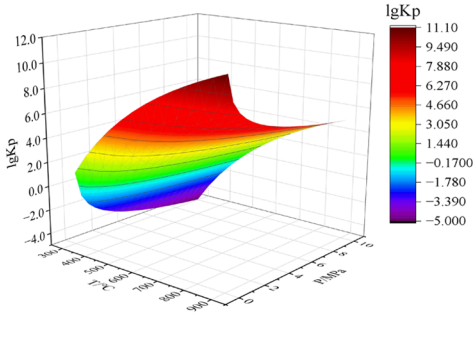

$C_6H_{11}CH_3=C_6H_5CH_3+3H_2$

(f) R12- Equilibrium constant

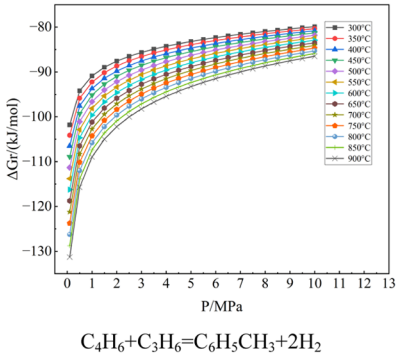

$C_4H_6+C_3H_6=C_6H_5CH_3+2H_2$

(g) R13-Gibbs free energy change

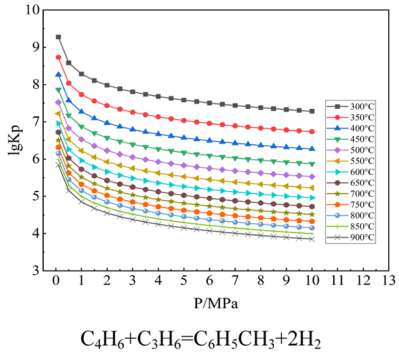

$C_4H_6+C_3H_6=C_6H_5CH_3+2H_2$

(h) R13- Equilibrium constant

Figure 2. Effects of temperature and pressure on the Gibbs free energy and equilibrium constant of R9 (a, b), R10 (c, d), R12 (e, f), and R13 (g, h).

tendency with increases in temperature and pressure.[46−48] This paper did not consider the effect of atmosphere on the reaction process, so the results obtained differed from those reported. It was found that the atmosphere had an important effect on the pyrolysis process. The secondary reaction was intensified with the increase in pressure and temperature. The hydrogen-rich

https://doi.org/10.1021/acsomega.2c08033
ACS Omega 2023, 8, 12805−12819

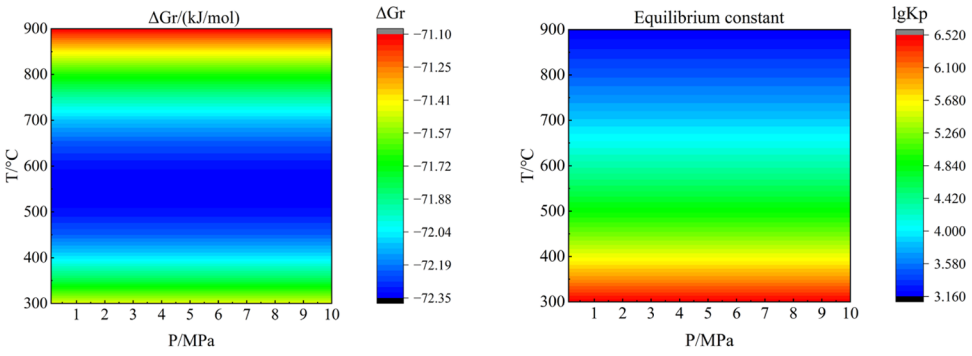

$C_6H_3(CH_3)_2OH+H_2=C_6H_4(CH_3)_2+H_2O$

(a) R14-Gibbs free energy change

$C_6H_3(CH_3)_2OH+H_2=C_6H_4(CH_3)_2+H_2O$

(b) R14- Equilibrium constant

Figure 3. Effects of temperature and pressure on the Gibbs free energy and equilibrium constant of R14 (a, b).

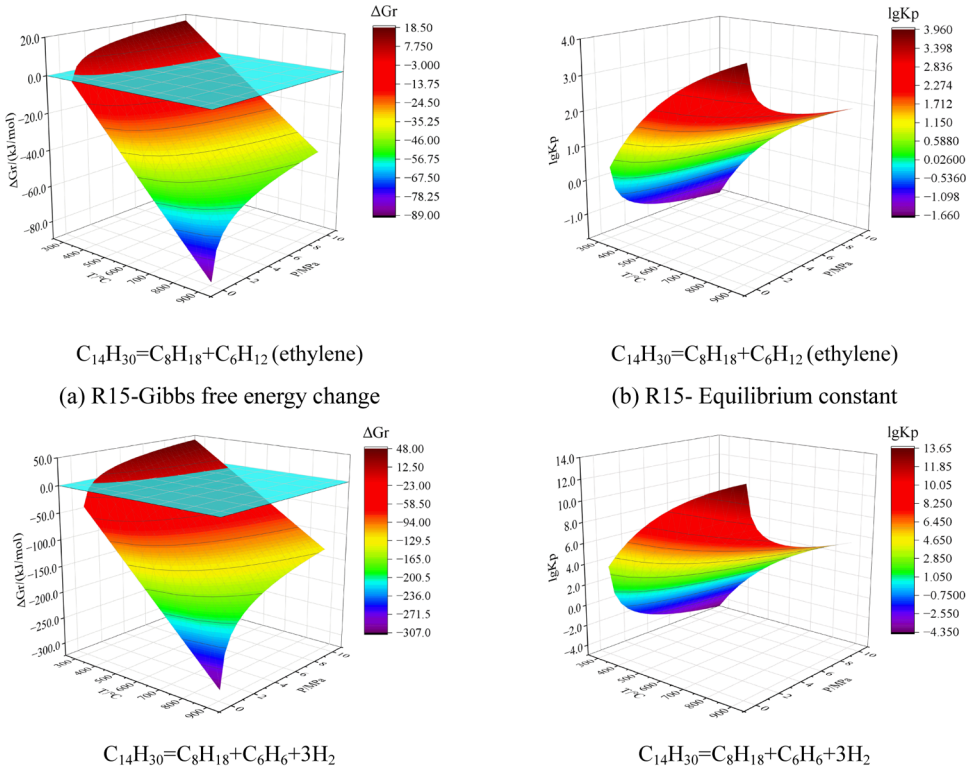

$C_{14}H_{30}=C_8H_{18}+C_6H_{12}$ (ethylene)

(a) R15-Gibbs free energy change

$C_{14}H_{30}=C_8H_{18}+C_6H_{12}$ (ethylene)

(b) R15- Equilibrium constant

$C_{14}H_{30}=C_8H_{18}+C_6H_6+3H_2$

(c) R17-Gibbs free energy change

$C_{14}H_{30}=C_8H_{18}+C_6H_6+3H_2$

(d) R17- Equilibrium constant

Figure 4. Effects of temperature and pressure on the Gibbs free energy and equilibrium constant of R15 (a, b) and R17 (c, d).

structures such as bridge bonds among benzene rings in macromolecular aromatic compounds and some alkyl side chains connected on the aromatic rings were cracked to release more benzene rings. In the pyrolysis process, the equimolecular reactions might be dominant, and the molecule-increasing reactions had little effect on benzene generation in tar.[49]

3.1.2. Secondary Reaction of Toluene as the Main Product. R8−R13 are secondary reactions with toluene as the main product. Figure 2 shows the changes in the Gibbs free energy and equilibrium constant of R9, R10, R12, and R13 with temperature and pressure. Relevant figures for R8 and R11 are provided in the Supporting Information. According to the relationship between the Gibbs free energy and temperature and pressure, the Gibbs free energy values of R8, R10, and R13 in the whole temperature and pressure ranges were all less than 0, and the reactions could be spontaneous. Under the same conditions, with the increase in pressure, the Gibbs free energy value of R13 gradually increased, and the trend in which the reaction could proceed spontaneously gradually weakened. Only when the temperature was below 385 °C, the Gibbs free energy value of R9 was less than 0, and the reaction could proceed spontaneously. At the atmospheric pressure, the Gibbs free energy values of R11 and R12 were less than 0 in the whole temperature range. The temperature nodes with the Gibbs free energy value were equal to 0 and gradually increased with increasing pressure. That is to say, when the pressure was high, R11 and R12 required higher temperatures to proceed spontaneously.

https://doi.org/10.1021/acsomega.2c08033
ACS Omega 2023, 8, 12805−12819

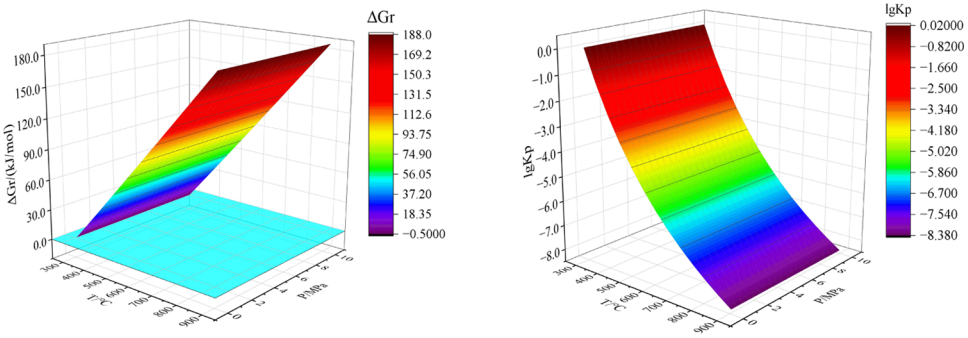

$C_6H_4CH_3OH+H_2=C_6H_5OH+CH_4$

(a) R18-Gibbs free energy change

$C_6H_4CH_3OH+H_2=C_6H_5OH+CH_4$

(b) R18- Equilibrium constant

Figure 5. Effects of temperature and pressure on the Gibbs free energy and equilibrium constant of R18 (a, b).

According to the relationship between the equilibrium constant and temperature and pressure, the equilibrium constants of R8, R9, R10, and R13 gradually decreased with increasing temperature, so they were exothermic reactions. Similarly, R11 and R12 were endothermic reactions. R8−R10 were equimolecular reactions, and R11−R13 were molecule-increasing reactions. Macroscopically, the increases in temperature and pressure were not conducive to the forward progress of the secondary reactions to generate toluene. Still, our findings were in substantial disagreement with those reported. They have shown that in a reducing atmosphere, such as H_2 or gas, increases in pressure and temperature could increase the toluene content in tar.[46,48] The difference between the conclusions might be attributed to the fact that in the actual pyrolysis process, the bridge bonds inside the macromolecular polycyclic aromatic hydrocarbons and the alkyl side chains attached to the aromatic rings themselves were thermally broken, resulting in more molecular chain ends. With increasing temperature, the methyl and aromatic ring radicals combined to generate toluene would intensify the secondary cracking of polycyclic aromatic hydrocarbons and the substitution reaction of aromatic carbon. The increasing pressure would prolong the residence time of tar molecules in the coal seam. Although the increase in pressure was not conducive to the molecule-increasing reaction, the cracking and substitution reactions proceeded more thoroughly due to the longer residence time. The reducing atmosphere could also promote the stabilization of free radical hydrogenation, which generally increases the toluene content in tar.

3.1.3. Secondary Reaction of Xylene as the Main Product. R14 is a secondary reaction with xylene as the main product. Figure 3 shows the Gibbs free energy change and equilibrium constant of R14 with temperature and pressure. According to the relationship between the Gibbs free energy and temperature and pressure, with the increase in temperature, the Gibbs free energy value of R14 was less than 0 in the whole temperature and pressure range, and the reaction could proceed spontaneously. According to the relationship between the equilibrium constant and temperature and pressure, the equilibrium constant of R14 gradually decreased with the increase in temperature, so it was an exothermic reaction. R14 was an equimolecular reaction. Macroscopically, the pressure did not affect the reaction of R14, and the increase in temperature was not conducive to the forward progress of the secondary reaction to generate xylene. Still, related scholars have shown that in the syngas atmosphere, the xylene content in tar increased with increasing pressure.[47] In the actual pyrolysis process, the generating mechanism of xylene was similar to that of toluene. With the increase in pressure and temperature, the secondary cracking, side-chain substitution, and hydrogenation reaction of macromolecular polycyclic aromatic hydrocarbons were intensified, the unstable bridge bonds in molecules were broken, and the contents of benzene ring free radicals and short aliphatic chain free radicals increased; they were more likely to combine, resulting in more xylene being produced.

3.1.4. Secondary Reaction of Octane as the Main Product. R15−R17 are secondary reactions with octane as the main product. Figure 4 shows the changes in the Gibbs free energy and equilibrium constant of R15 and R17 with temperature and pressure. A relevant figure for R16 is provided in the Supporting Information. According to the relationship between the Gibbs free energy and temperature and pressure, at the atmospheric pressure, the Gibbs free energy values of R15 and R17 were less than 0 in the whole temperature range. With the increase in pressure, the temperature nodes with Gibbs free energy values equal to 0 gradually increased, so when the pressure was high, R15 and R17 required higher temperatures to proceed spontaneously. The Gibbs free energy value of R16 was less than 0 in the whole temperature and pressure range, so the reaction could proceed spontaneously. However, the Gibbs free energy value increased gradually at the same temperature with increasing pressure. The trend that the reaction could proceed spontaneously gradually weakened.

According to the relationship between the equilibrium constant and temperature and pressure, with increasing temperature, the equilibrium constants of R15 and R17 gradually increased, so they were endothermic reactions. Similarly, R16 was an exothermic reaction. All three reactions were molecule-increasing reactions. Macroscopically, the increase in pressure was not conducive to the forward progress of the reactions, and an increase in the temperature could promote the forward progress of the secondary reactions to generate octane. In the actual pyrolysis process, when the pressure and temperature increased, the secondary cracking of the macromolecular long-chain aliphatic hydrocarbon side chains and the polymerization among the small molecular hydrocarbon radicals intensified; this led to the generation of more low-carbon hydrocarbons.

https://doi.org/10.1021/acsomega.2c08033
ACS Omega 2023, 8, 12805−12819

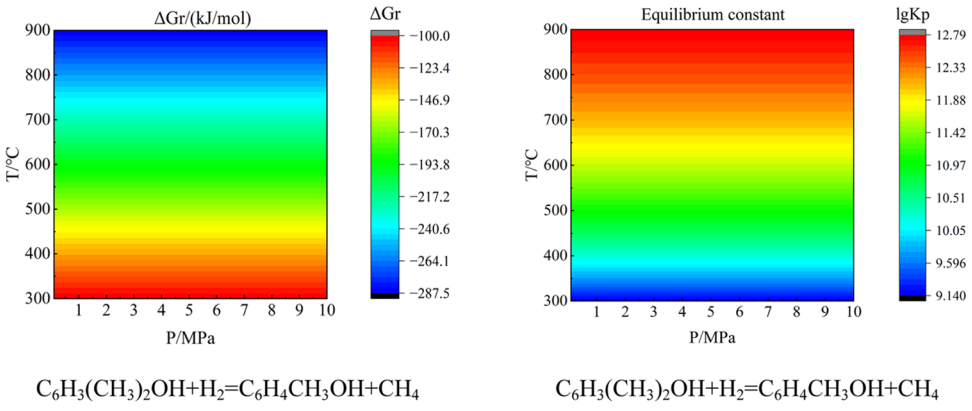

$C_6H_3(CH_3)_2OH+H_2=C_6H_4CH_3OH+CH_4$

(a) R19-Gibbs free energy change

$C_6H_3(CH_3)_2OH+H_2=C_6H_4CH_3OH+CH_4$

(b) R19- Equilibrium constant

Figure 6. Effects of temperature and pressure on the Gibbs free energy and equilibrium constant of R19 (a, b).

3.2. Thermodynamic Analysis of Secondary Reactions to Generate Phenol Tar. *3.2.1. Secondary Reaction with Phenol as the Main Product.* R18 is a secondary reaction with phenol as the main product. Figure 5 shows the Gibbs free energy change and equilibrium constant of R18 with temperature and pressure. According to the relationship between the Gibbs free energy and temperature and pressure, the Gibbs free energy value of R18 was less than 0, only below 301 °C. The Gibbs free energy value was greater than 0 in other temperature ranges, so the temperature range studied in this paper was not conducive to the spontaneous progress of R18. According to the relationship between the equilibrium constant and temperature and pressure, the equilibrium constant of R18 decreased with increasing temperature, so it was an exothermic reaction. R18 was an equimolecular reaction. Macroscopically, the pressure did not affect the reaction of R18, and the increase in temperature was not conducive to the forward progress of the secondary reaction to generate phenol.

In contrast, the results reported in the literature appeared to refute the obtained results. They have shown that in the reducing atmosphere, pressurization was conducive to phenol generation.[46,47] The generating mechanism of phenol in the actual pyrolysis process was similar to that of benzene and toluene. The secondary cracking was intensified with the increase in temperature and pressure, and the macromolecular polyphenol compounds were cracked to generate monocyclic phenols. The combination probability of hydroxyl radicals and aromatic carbon radicals increased, and the phenol content in tar increased.

3.2.2. Secondary Reaction with Cresol as the Main Product. R19 is a secondary reaction with cresol as the main product. Figure 6 shows the change of Gibbs free energy and equilibrium constant of R19 with temperature and pressure. According to the relationship between the Gibbs free energy and temperature and pressure, the Gibbs free energy value of R19 was less than 0 in the entire temperature and pressure range, and the reaction could be carried out spontaneously. According to the relationship between the equilibrium constant and temperature and pressure, the equilibrium constant continued to increase with increasing temperature, so R19 was an endothermic reaction. Also, R19 was an equimolecular reaction. Macroscopically, the pressure did not affect the reaction of R19, and the increasing temperature was conducive to the forward progress of the secondary reaction to generate cresol. Still, the results were inconsistent with those reported in the literature. The reports have shown that tar's cresol content in the coke oven gas atmosphere increased with increasing pressure.[45] In the actual pyrolysis process, the residence time of volatiles in the coal seam became longer with increasing pressure. The crackings of bridge bonds, side chains, and oxygen-containing functional groups in macromolecular aromatic rings were intensified. The contents of methyl and hydroxyl radicals increased, and their binding probability with aromatic rings increased, resulting in an increase in cresol content in tar.

3.3. Thermodynamic Analysis of Secondary Reactions to Generate Naphthalene Tar. *3.3.1. Secondary Reactions with Naphthalene as the Main Product.* R20−R25 are the secondary reactions with naphthalene as the main product. Figure 7 shows the changes in the Gibbs free energy and equilibrium constants of R23−R25 with temperature and pressure. Relevant figures for R20−R22 are provided in the Supporting Information. According to the relationship between the Gibbs free energy and temperature and pressure, the Gibbs free energy values of R21−R24 were less than 0 in the entire temperature and pressure range, and the reactions could proceed spontaneously. However, with the increase in pressure, the Gibbs free energy values increased gradually at the same temperature. The trend in which the reactions could proceed spontaneously gradually weakened. With the increased pressure, the temperature range in which R20 could spontaneously proceed progressively narrowed. The Gibbs free energy value of R25 in the entire temperature and pressure range was less than 0. The reaction could proceed spontaneously.

According to the relationship between the equilibrium constant and temperature and pressure, the equilibrium constants of R20, R21, R23, R24, and R25 gradually decreased with increasing temperature, so they were exothermic reactions. Similarly, R22 was an endothermic reaction. R20−R24 were all molecule-increasing reactions. Due to the semi-coke produced being solid particles, R25 could be regarded as an equimolecular reaction. Macroscopically, the increases in pressure and temperature were not conducive to the forward progress of the secondary reaction to generate naphthalene. Still, the reports in the literature have shown that the naphthalene content in tar gradually increased with increasing pressure in the coke oven gas atmosphere.[46,47] In the pyrolysis process, naphthalene was mainly generated by the polymer-

https://doi.org/10.1021/acsomega.2c08033
ACS Omega 2023, 8, 12805−12819

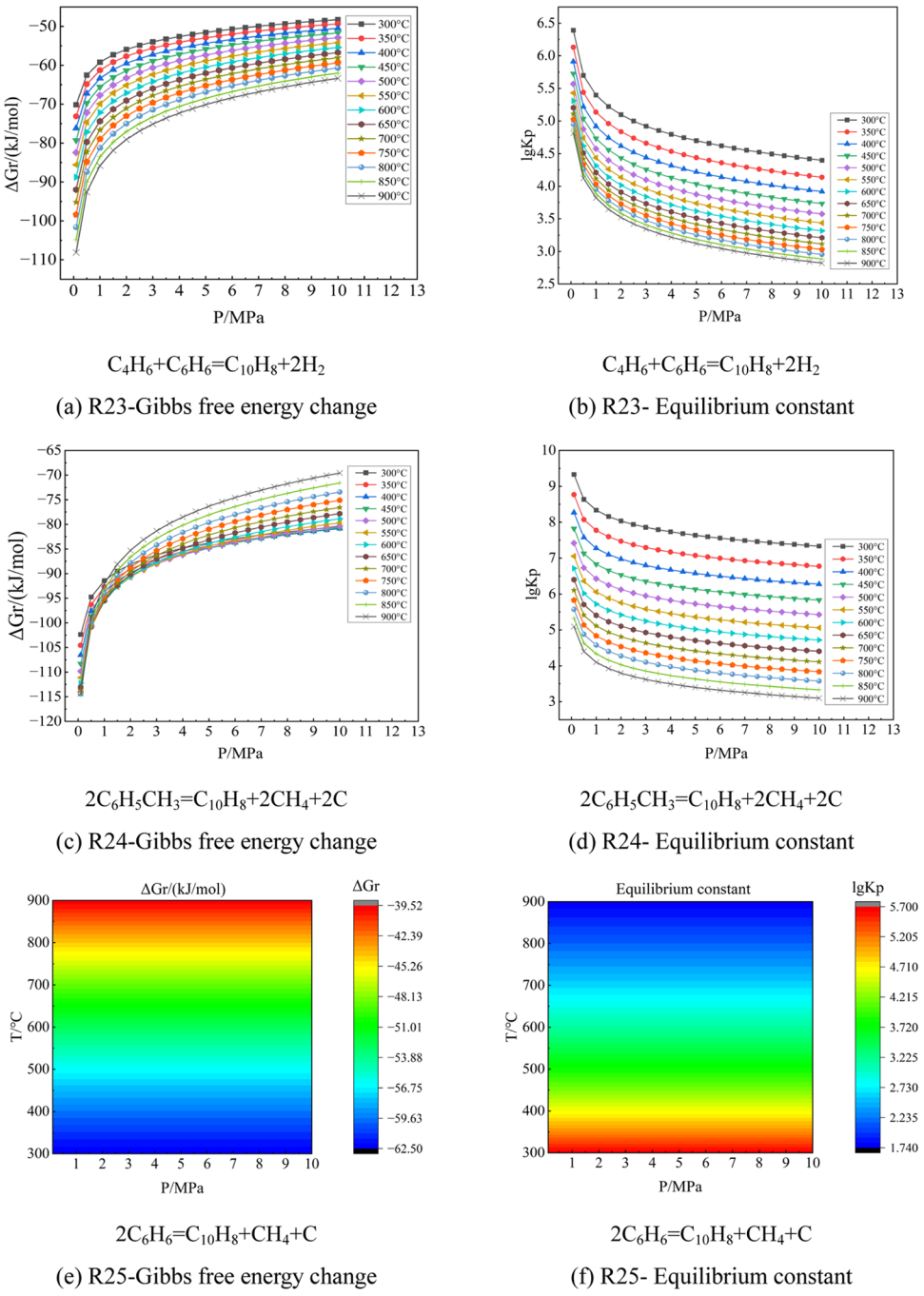

$C_4H_6+C_6H_6=C_{10}H_8+2H_2$

(a) R23-Gibbs free energy change

$C_4H_6+C_6H_6=C_{10}H_8+2H_2$

(b) R23- Equilibrium constant

$2C_6H_5CH_3=C_{10}H_8+2CH_4+2C$

(c) R24-Gibbs free energy change

$2C_6H_5CH_3=C_{10}H_8+2CH_4+2C$

(d) R24- Equilibrium constant

$2C_6H_6=C_{10}H_8+CH_4+C$

(e) R25-Gibbs free energy change

$2C_6H_6=C_{10}H_8+CH_4+C$

(f) R25- Equilibrium constant

Figure 7. Effects of temperature and pressure on the Gibbs free energy and equilibrium constant of R23 (a, b), R24 (c, d), and R25 (e, f).

ization of some monocyclic phenols or monocyclic aromatic compounds and the cracking of macromolecular polycyclic aromatic hydrocarbons. When the pressure was high, the precipitation of tar molecules was difficult, the residence time in the coal seam became longer, and the secondary reactions among free radicals were intensified. Also, the polymerization of monocyclic phenols and aromatic substances and the cracking of polycyclic aromatic hydrocarbons were both promoted. The increase in temperature accelerated the rate of a secondary reaction. It could also promote the partial endothermic secondary reactions to proceed forward, resulting in increased naphthalene content in tar.

3.3.2. Secondary Reactions with N-Dodecane as the Main Product. R26 is a secondary reaction with *n*-dodecane as the main product. Figure 8 shows the change of the Gibbs free energy and equilibrium constant of R26 with temperature and pressure. According to the relationship between the Gibbs free energy and temperature and pressure, the Gibbs free energy value of R26 was less than 0 in the whole temperature and pressure range, and the reaction could proceed spontaneously. However, with the increase in pressure, the Gibbs free energy value increased gradually at the same temperature, and the trend in which the reaction could proceed spontaneously gradually weakened. According to the relationship between the equilibrium constant and temperature and pressure, the equilibrium constant of R26 gradually decreased with increasing temperature, so it was an exothermic reaction. R26 was a molecule-increasing reaction. Macroscopically, the

https://doi.org/10.1021/acsomega.2c08033
ACS Omega 2023, 8, 12805−12819

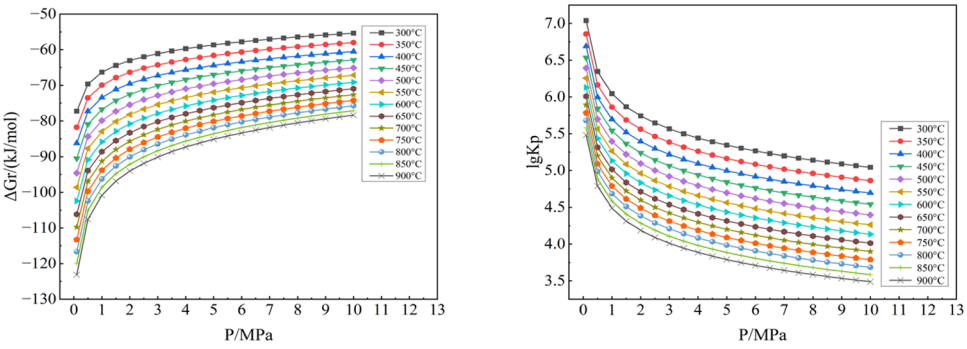

$C_{14}H_{30}=C_{12}H_{26}+CH_4+C$ $C_{14}H_{30}=C_{12}H_{26}+CH_4+C$

(a) R26-Gibbs free energy change (b) R26- Equilibrium constant

Figure 8. Effects of temperature and pressure on the Gibbs free energy and equilibrium constant of R26 (a, b).

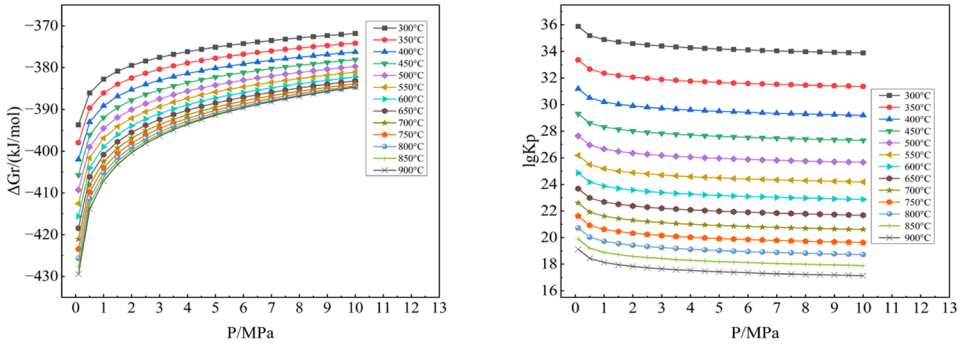

$C_6H_5CH_3+C_6H_4CH_3OH=C_{11}H_{10}+CH_4+H_2O+2C$ $C_6H_5CH_3+C_6H_4CH_3OH=C_{11}H_{10}+CH_4+H_2O+2C$

(a) R27-Gibbs free energy change (b) R27- Equilibrium constant

Figure 9. Effects of temperature and pressure on the Gibbs free energy and equilibrium constant of R27 (a, b).

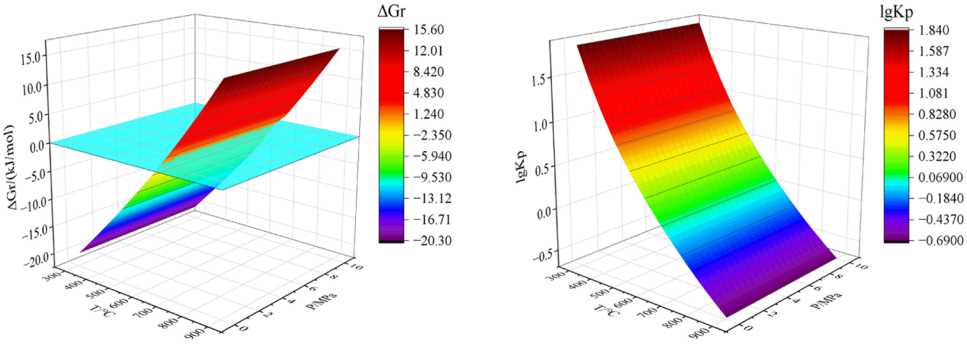

$2C_6H_5CH_3=C_{12}H_{12}+CH_4+C$ $2C_6H_5CH_3=C_{12}H_{12}+CH_4+C$

(a) R28-Gibbs free energy change (b) R28- Equilibrium constant

Figure 10. Effects of temperature and pressure on the Gibbs free energy and equilibrium constant of R28 (a, b).

increases in pressure and temperature were not conducive to the forward progress of the secondary reaction to generate *n*-dodecane. In the pyrolysis process, *n*-dodecane was mainly obtained by polymerizing small molecular hydrocarbon free radicals and cracking macromolecular long-chain alkanes. Due to the large molecular weight and long carbon chain of *n*-dodecane itself, it could also be decomposed into small molecular free radicals under certain conditions. Therefore, the temperature, pressure, and pyrolysis atmosphere should be reasonably determined according to the actual needs to obtain the tar containing *n*-dodecane with the ideal content.

3.4. Thermodynamic Analysis of Secondary Reactions to Generate Washing Tar. *3.4.1. Secondary Reaction with Methylnaphthalene as the Main Product.* R27 is a secondary reaction with methylnaphthalene as the main product. Figure 9 shows the changes of the Gibbs free energy and equilibrium constant of R27 with temperature and pressure. According to the relationship between the Gibbs free energy and temperature and pressure, the Gibbs free

https://doi.org/10.1021/acsomega.2c08033
ACS Omega 2023, 8, 12805−12819

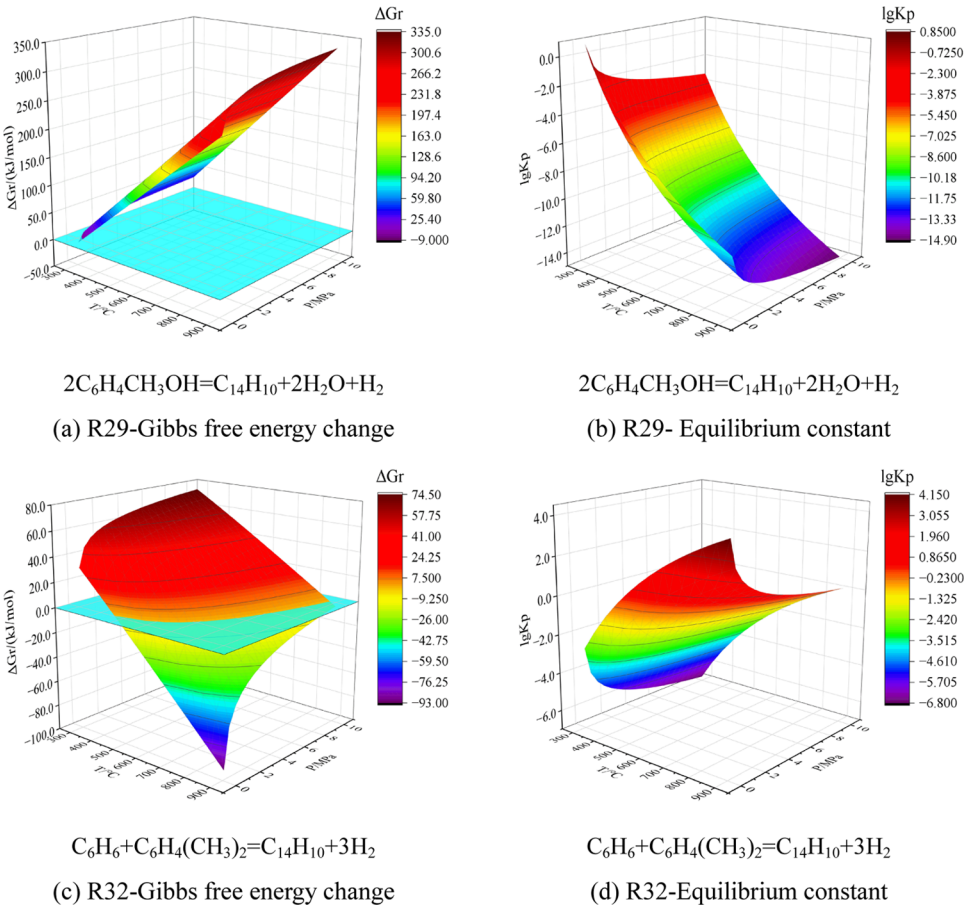

$2C_6H_4CH_3OH=C_{14}H_{10}+2H_2O+H_2$

(a) R29-Gibbs free energy change

$2C_6H_4CH_3OH=C_{14}H_{10}+2H_2O+H_2$

(b) R29- Equilibrium constant

$C_6H_6+C_6H_4(CH_3)_2=C_{14}H_{10}+3H_2$

(c) R32-Gibbs free energy change

$C_6H_6+C_6H_4(CH_3)_2=C_{14}H_{10}+3H_2$

(d) R32-Equilibrium constant

Figure 11. Effects of temperature and pressure on the Gibbs free energy and equilibrium constant of R29 (a, b) and R32 (c, d).

energy value of R27 was less than 0 in the whole temperature and pressure range. The reaction could proceed spontaneously. However, with increasing pressure, the Gibbs free energy value gradually increased at the same temperature. The trend in which the reaction could proceed spontaneously gradually weakened. According to the relationship between the equilibrium constant and temperature and pressure, the equilibrium constant of R27 decreased gradually with increasing temperature, so it was an exothermic reaction. R27 was a molecule-increasing reaction. Macroscopically, the increases in pressure and temperature were not conducive to the forward progress of the secondary reaction to generate methylnaphthalene. Still, the study has indicated that in a H_2 atmosphere, with the temperature increase, the methylnaphthalene content in tar increased first and then decreased. Under the same conditions, methylnaphthalene content increased gradually with increasing pressure.[48] Due to the exothermic reaction, when the temperature was low, the reaction rate increased with increasing temperature, so the yield of methylnaphthalene increased. However, when the temperature was too high, the forward progress of the reaction was inhibited, and the yield of methylnaphthalene was decreased. Methylnaphthalene was mainly generated by polymerizing methyl radicals and aromatic carbon radicals. The increases in pressure and temperature aggravated the cracking of aromatic ring side chains and the activation of aromatic carbons. The probability of free radicals contacting each other was increased. Therefore, the methylnaphthalene content in tar was also increased.

3.4.2. Secondary Reaction with Dimethylnaphthalene as the Main Product. R28 is a secondary reaction with dimethylnaphthalene as the main product. Figure 10 shows the change of the Gibbs free energy and equilibrium constant of R28 with temperature and pressure. According to the relationship between the Gibbs free energy and temperature and pressure, in the whole pressure range, only when the temperature was lower than 666 °C, the Gibbs free energy value of R28 was less than 0, and the reaction could proceed spontaneously. According to the relationship between the equilibrium constant and temperature and pressure, the equilibrium constant of R28 decreased with increasing temperature, so it was an exothermic reaction. Due to the semi-coke generated by the reaction being solid particles, R28 could be regarded as an equimolecular reaction. Macroscopically, the pressure did not affect the reaction. The increase in temperature was not conducive to the forward progress of the secondary reaction to generate dimethylnaphthalene. Dimethylnaphthalene was a bicyclic aromatic compound that could be obtained from the polymerization of monocyclic aromatic hydrocarbons and phenols or the cracking of macromolecular condensed aromatic hydrocarbons in the pyrolysis process. Its generation mechanism was similar to that of methylnaphthalene.

3.5. Thermodynamic Analysis of Secondary Reactions to Generate Anthracene Tar. R29−R32 are the secondary reactions with anthracene as the main product. Figure 11 shows the changes in the Gibbs free energy and equilibrium constant of R29 and R32 with temperature and

https://doi.org/10.1021/acsomega.2c08033
ACS Omega 2023, 8, 12805−12819

pressure. Relevant figures for R30 and R31 are provided in the Supporting Information. According to the relationship between the Gibbs free energy and temperature and pressure, at the atmospheric pressure, only when the temperature was below 321 °C, the Gibbs free energy value of R29 was less than 0, and the reaction could proceed spontaneously. In other temperature and pressure ranges, the Gibbs free energy value was greater than 0, and the reaction could not proceed spontaneously. So, in the temperature and pressure range studied in this paper, R29 basically could not proceed spontaneously. The Gibbs free energy value of R30 in the entire temperature and pressure range was less than 0. The reaction could proceed spontaneously. However, the Gibbs free energy value gradually increased with increasing pressure, so the tendency of the reaction to move spontaneously weakened. With the increase in pressure, the temperature nodes with the Gibbs free energy values of R31 and R32 were equal to 0 and gradually increased. The initial temperature of the two reactions could be spontaneously increased progressively.

According to the relationship between the equilibrium constant and temperature and pressure, the equilibrium constants of R29 and R30 gradually decreased with increasing temperature, so they were exothermic reactions. Similarly, R31 and R32 were endothermic reactions. R29−R32 were molecule-increasing reactions. Macroscopically, the increase in pressure was not conducive to the forward progress of the secondary reactions to generate anthracene. The effect of temperature on the generation of anthracene should be analyzed according to the specific situation. Anthracene is a tricyclic aromatic hydrocarbon, which could be obtained by the polymerization of monocyclic or bicyclic aromatic hydrocarbons and phenols. Also, it could be generated by the cracking of macromolecular polycyclic aromatic hydrocarbons. Due to the large molecular weight of anthracene, polymerization or cracking could both occur at specific temperature and pressure conditions. So, in the actual production process, the pyrolysis conditions should be reasonably selected according to the actual needs to adjust the anthracene content in tar.

3.6. Summary of the Relationship between Initial Temperature and Pressure for the Reactions to Proceed Spontaneously. From Figure 12, although the main components contained in the light tar and anthracene tar were different, each typical secondary reaction mechanism and reaction conditions were also different. However, with the increase in pressure, the initial temperature at which typical secondary reactions with benzene, toluene, octane, and anthracene as the main products could proceed spontaneously increased gradually. Except for the above seven reactions, the Gibbs free energy values of other molecule-increasing reactions in the entire temperature and pressure range were less than 0, and the reactions could proceed spontaneously. However, the Gibbs free energy value gradually increased with increasing pressure, and the tendency for the reactions to proceed spontaneously progressively weakened. In conclusion, the increase in pressure was detrimental to the forward proceeding of the molecule-increasing reactions.

4. CONCLUSIONS

This paper analyzes the thermodynamic characteristics of typical secondary reactions during *in situ* underground pyrolysis of tar-rich coal. Pressure mainly affected the

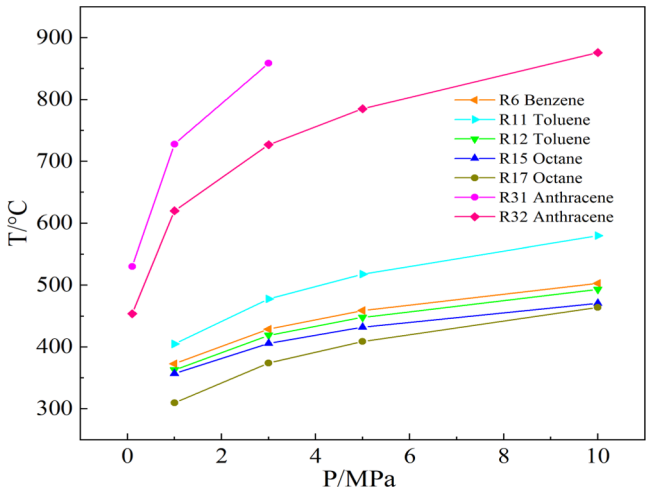

Figure 12. Thermodynamically feasible initial temperature versus pressure for the reactions.

molecule-increasing reactions. The initial temperature at which these reactions could proceed spontaneously gradually increased, or the Gibbs free energy value gradually increased with increasing pressure. Macroscopically, for light tar, the secondary reactions with benzene, toluene, and octane as the main reaction products contained some molecule-increasing reactions, and the secondary reaction with xylene as the main reaction product was an equimolecular reaction. Hence, the increase in pressure was not conducive to the generation of benzene, toluene, and octane. It did not affect the generation of xylene. For R6 with benzene as the main product, R11 and R12 with toluene as the main product, and R15 and R17 with octane as the main product, when the pressure was 0.1 MPa, the Gibbs free energy of these reactions was less than 0 in the whole temperature range, and the reactions could proceed spontaneously. When the pressure increased from 0.1 to 10 MPa, the initial temperature at which the reactions could proceed spontaneously increased to 503, 580, 493, 471, and 464 °C, respectively. The increase in temperature could promote the generation of octane, but it was not conducive to the generation of benzene, toluene, and xylene. The secondary reactions with phenol and cresol as the main reaction products for phenol tar were all equimolecular reactions. So, the generation of phenol and cresol was not affected by pressure. The increasing temperature could promote the generation of cresol, but it was not conducive to the generation of phenol. For the naphthalene tar, due to the secondary reactions with naphthalene as the main reaction products containing some molecule-increasing reactions, the secondary reaction with *n*-dodecane as the main reaction product was equimolecular. So, the increases in pressure and temperature were not conducive to the generation of naphthalene, and it had no effect on the generation of *n*-dodecane. For the washing tar, due to the secondary reaction with methylnaphthalene as the main reaction product being a molecule-increasing reaction, the secondary reaction with dimethylnaphthalene as the main reaction product was an equimolecular reaction. So, the increase in pressure was not conducive to the generation of methylnaphthalene, and it did not affect the generation of dimethylnaphthalene. The increasing temperature was not conducive to the generation of both methylnaphthalene and dimethylnaphthalene. For the anthracene tar, the secondary reactions with anthracene as the main reaction product were all

https://doi.org/10.1021/acsomega.2c08033
ACS Omega 2023, 8, 12805−12819

molecule-increasing reactions. So, the increase in pressure was not conducive to the generation of anthracene. For R31 with anthracene as the main product, when the pressure increased from 0.1 to 3 MPa, the initial temperature for reaction could proceed spontaneously, increasing from 530 to 859 °C. When the pressure was higher than 3 MPa, the reaction could spontaneously proceed in the whole temperature range. For R32 with anthracene as the main product, when the pressure increased from 0.1 to 10 MPa, the initial temperatures for reaction could proceed spontaneously, increasing from 454 to 876 °C. The effect of temperature on the generation of anthracene should be analyzed in combination with the actual situation.

■ ASSOCIATED CONTENT

Supporting Information

The Supporting Information is available free of charge at https://pubs.acs.org/doi/10.1021/acsomega.2c08033.

Gibbs free energy change of each reaction; equilibrium constant of each reaction, and effects of temperature and pressure on Gibbs free energy and equilibrium constant of some secondary reactions (PDF)

■ AUTHOR INFORMATION

Corresponding Author

Zhiqiang Wu − *Shanxi Key Laboratory of Energy Chemical Process Intensification, School of Chemical Engineering and Technology, Xi'an Jiaotong University, Xi'an, Shaanxi 710049, China*; orcid.org/0000-0002-3067-014X; Phone: +86-29-82665836; Email: zhiqiang-wu@mail.xjtu.edu.cn

Authors

Deliang Fu − *Key Laboratory of Coal Resources Exploration and Comprehensive Utilization, Ministry of Natural and Resources, Shaanxi Provincial Coal Geology Group Co., Ltd., Xi'an 710026, China*

Zunyi Yu − *Shanxi Key Laboratory of Energy Chemical Process Intensification, School of Chemical Engineering and Technology, Xi'an Jiaotong University, Xi'an, Shaanxi 710049, China*

Kun Gao − *Shanxi Key Laboratory of Energy Chemical Process Intensification, School of Chemical Engineering and Technology, Xi'an Jiaotong University, Xi'an, Shaanxi 710049, China*

Zhonghui Duan − *Key Laboratory of Coal Resources Exploration and Comprehensive Utilization, Ministry of Natural and Resources, Shaanxi Provincial Coal Geology Group Co., Ltd., Xi'an 710026, China*

Zhendong Wang − *Key Laboratory of Coal Resources Exploration and Comprehensive Utilization, Ministry of Natural and Resources, Shaanxi Provincial Coal Geology Group Co., Ltd., Xi'an 710026, China*

Wei Guo − *Shanxi Key Laboratory of Energy Chemical Process Intensification, School of Chemical Engineering and Technology, Xi'an Jiaotong University, Xi'an, Shaanxi 710049, China*

Panxi Yang − *Shanxi Key Laboratory of Energy Chemical Process Intensification, School of Chemical Engineering and Technology, Xi'an Jiaotong University, Xi'an, Shaanxi 710049, China*

Jie Zhang − *Shanxi Key Laboratory of Energy Chemical Process Intensification, School of Chemical Engineering and Technology, Xi'an Jiaotong University, Xi'an, Shaanxi 710049, China*

Bolun Yang − *Shanxi Key Laboratory of Energy Chemical Process Intensification, School of Chemical Engineering and Technology, Xi'an Jiaotong University, Xi'an, Shaanxi 710049, China*

Fu Yang − *Key Laboratory of Coal Resources Exploration and Comprehensive Utilization, Ministry of Natural and Resources, Shaanxi Provincial Coal Geology Group Co., Ltd., Xi'an 710026, China*

Complete contact information is available at: https://pubs.acs.org/10.1021/acsomega.2c08033

Author Contributions

§D.F. and Z.Y. contributed equally to this work.

Notes

The authors declare no competing financial interest.

■ ACKNOWLEDGMENTS

The financial support from the Research Project of Shaanxi Provincial Coal Geology Group Co., Ltd., (No. SMDZ-2020ZD-1-02), the K.C. Wang Education Foundation, Shaanxi Province Qin Chuangyuan "Scientist + Engineer" team development project (No. 2022KXJ-126), and Innovation Capability Support Program of Shaanxi (Nos. 2022KJXX-24 and 2023SR5005) is acknowledged.

■ SYMBOL DESCRIPTION

C_p, heat capacity, J (kg K)$^{-1}$; ΔG, Gibbs free energy change; $\Delta_r G_m^\theta$, standard formation Gibbs free energy change, kJ mol^{-1}; $\Delta_r H_m^\theta$, standard enthalpy change of formation, kJ mol^{-1}; $\Delta_r H_m$, enthalpy change of the reaction, kJ mol^{-1}; M_a, average molecular weight of coal; n, amount of substance, mol; P, pressure, MPa; p^θ, standard atmospheric pressure, 0.1 MPa; R, gas molar constant, 8.314 J (mol K)$^{-1}$; S, entropy, J (mol K)$^{-1}$; $\Delta_r S_m^\theta$, standard entropy change, J (mol K)$^{-1}$; V, volume, dm^3; θ, standard status; a, average; i, component; r, reactive state; m, mol

■ REFERENCES

(1) Li, J. F.; Li, G. Review and outlook on energy, environment and climate change in China [J]. *Environ. Sustainable Dev.* **2020**, *45*, 8−17.

(2) Wang, X. L.; Chen, G. F.; Li, W. B.; Huang, P.; Wang, N. J. Construction of the direction of clean and efficient utilization of coal under the background of double carbon [J]. *Coal Qual. Technol.* **2021**, *36*, 1−5.

(3) Krumm, R. L.; Gneshin, K. W.; Deo, M. Adsorption Characteristics of Coals Pyrolyzed at Slow Heating Rates [J]. *Energy Fuels* **2017**, *31*, 1803−1810.

(4) Li, H. B.; Yao, Z.; Li, N.; Gao, J.; Xie, Q.; Wang, Q. Evaluation of tar-rich coal deposit characteristics and resource potential of the 5∼(-2) coal seam in Shen Fu mining area [J]. *Coal Geol. Explor.* **2021**, *49*, 26−32.

(5) Wang, S. M.; Shi, Q. M.; Wang, S. Q.; Shen, Y. J.; Sun, Q.; Cai, Y. Tar and gas resource properties of tar-rich coal and green low-carbon development [J]. *J. China Coal Soc.* **2021**, *46*, 1365−1377.

(6) Zhang, L.; Han, Z. K.; Shu, H.; Jia, Y.; Kuang, W.; Sun, Z. Y.; Song, S. Y. Basic characteristics of low-temperature pyrolysis of oil-rich coal in northern Shaanxi [J]. *Coal Eng.* **2022**, *54*, 124−128.

(7) Li, Y. Coal structure evolution and development of fuel, raw material and material properties [J/OL]. *J. China Coal Soc.* 1 16.

(8) Zhang, H. Z. R.; Li, S. H.; Kelly, K. E.; Eddings, E. G. Underground in situ coal thermal treatment for synthetic fuels production [J]. *Prog. Energy Combust. Sci.* **2017**, *62*, 1−32.
(9) Guo, S. C.; Hu, H. Q. *Coal Chemical Technology [M]*; Chemical Industry Press Co., Ltd., 2012.
(10) Wu, Z. Q.; Guo, W.; Zhang, J.; Yang, B. L.; Wei, J. J.; Li, M. J. A method of preparing and using a catalytic module for underground in-situ pyrolysis of coal [P]. CN Patent CN202010987908ZL2021. September 07, 2021.
(11) Wu, Z. Q.; Guo, W.; Zhang, J.; Li, M. J.; Yang, B. L.; Wei, J. J. A preparation method and filling method of proppant used for coal underground in-situ pyrolysis [P]. CN Patent CN202010992622ZL2021. December 28, 2021.
(12) Wu, Z. Q.; Zhang, J.; Guo, W.; Yang, B. L.; Li, M. J.; Wei, J. J. A well layout structure and construction method for underground in-situ pyrolysis of coal [P]. CN Patent CN202010987906ZL2021. December 28, 2021.
(13) Wu, Z. Q.; Zhang, J.; Yang, B. L.; Guo, W.; Zhang, R. J.; Li, M. J.; Wei, J. J. A system and method for underground in-situ pyrolysis of coal [P]. CN Patent CN202010991619ZL2021. December 28, 2021.
(14) Wu, Z. Q.; Zhang, J.; Guo, W.; Yang, B. L.; Li, M. J.; Wei, J. J. A closed system for underground in-situ pyrolysis of coal and its construction method [P]. CN Patent CN2020109916182021. February 26, 2021.
(15) Wang, P. F.; Jin, L. J.; Liu, J. H.; Zhu, S. W.; Hu, H. Q. Analysis of coal tar derived from pyrolysis at different atmospheres [J]. *Fuel* **2013**, *104*, 14−21.
(16) Chareonpanich, M.; Takeda, T.; Yamashita, H.; Tomita, A. Catalytic hydrocracking reaction of nascent coal Volatile matter under high pressure [J]. *Fuel* **1994**, *73*, 666−670.
(17) Zu, J. R.; Li, K. Z.; Liu, L.; Gao, Z. Y.; Wang, H. F.; Mao, Y. D.; Lu, T.; Wu, H. Pressurized catalytic pyrolysis characteristics of Buliangou coal [J]. *Coal Convers.* **2018**, *41*, 19−25.
(18) Liang, Y. H.; Zhang, B. F.; Liu, Z. L. Study on pyrolysis characteristics of coal pressurized in fixed bed [J]. *J. Wuhan Iron Steel Univ.* **1990**, *01*, 68−75.
(19) Liu, X. Z.; Pang, J. Study on composition and properties of tar obtained by pressurized pyrolysis of Gansu Tianzhu coal [J]. *Coal Convers.* **1994**, *01*, 82−88.
(20) Smith, P. J.; Deo, M.; Edding, E. G.; Hradisky, M.; Kelly, K. E.; Krumm, R. *Undergroundcoal Thermal Treatment - Task 6 Topical Report, Utah Clean Coal Program [J]*, Content.lib.utah.edu, 2014.
(21) Wang, K. *Study on the Secondary Reactions of Volatile Fraction Obtained from the Pyrolysis of Shendong Coal through the Semi-Coke Layer [D]*; Northwestern University, 2018.
(22) Zhang, Y. M.; Guan, J. T.; Qiao, P.; Zhou, Li. Jia.; Zhang, W. Effects of secondary reaction of tar shale pyrolysis volatile products on tar and gas yield and composition [J]. *J. Fuel Chem. Technol.* **2021**, *49*, 924−932.
(23) Chen, Y. L.; He, R. Modeling of secondary reactions during coal pyrolysis [J]. *J. Tsinghua Univ. (Sci. Technol.)* **2011**, *51*, 672−676.
(24) Dun, Q. M. *Study on the Secondary Reaction Characteristics of Volatile Components in Coal Pyrolysis [D]*; Hebei University of Technology, 2017.
(25) Katheklakis, I. E.; Lu, S. L.; Bartle, K. D.; Kandiyoti, R. Effect of freeboard residence time on the molecular Mass distributions of fluidized bed pyrolysis tars [J]. *Fuel* **1990**, *69*, 172−176.
(26) Hayashi, J.; Nakagawa, K.; Kusakabe, K.; Morooka, S.; Yumura, M. Change in molecular structure of flash pyrolysis tar by secondary reaction in a fluidized bed reactor [J]. *Fuel Process. Technol.* **1992**, *30*, 237−248.
(27) Ariunaa, A.; Bao-Qing, L. I.; Wen, L. I.; Purevsuren, B.; Sh, M.; Liu, F. R.; Bai, Z. Q.; Wang, G. Coal pyrolysis under synthesis gas, hydrogen and nitrogen [J]. *J. Fuel Chem. Technol.* **2007**, *35*, 1−4.
(28) Gao, C.; Ma, F. Y.; Ma, K. J.; Huang, L. M.; Zhong, M. Effect of pyrolysis atmosphere on the quality of coal catalytic pyrolysis tar [J]. *J. China Coal Soc.* **2015**, *40*, 1956−1962.
(29) Xu, F. *Molecular Model Construction of Huolinhe Lignite and Molecular Dynamics Simulation of Its Pyrolysis Reaction [D]*; Harbin University of Technology, 2020.
(30) Hong, D. K.; Liu, L.; Guan, Z.; Yang, C. M.; Guo, X. Reactive Molecular Dynamics Study on Pyrolysis of Wucaiwan Coal [J]. *J. China Coal Soc.* **2019**, *44*, 271−277.
(31) Chen, Z. H.; Gao, S. Q.; Xu, G. W. Coal pyrolysis process analysis and process control method [J]. *CIESC J.* **2017**, *68*, 3693−3707.
(32) Chen, Y. F. *Effect of Gas Residence Time on the Release Products of Coal Pyrolysis in Fluidized Bed [D]*; Zhejiang University, 2017.
(33) Chen, Z. R. *Effect of Pyrolysis Gas Residence Time on Pyrolysis Products during Coal Pyrolysis [D]*; Zhejiang University, 2015.
(34) Hong, D. K. *Reactive Molecular Dynamics Study of Zhundong Coal Pyrolysis and Oxy-Fuel Combustion [D]*; Huazhong University of Science and Technology, 2018.
(35) Zheng, M.; Li, X.; Guo, L. Dynamic trends for char/soot formation during secondary reactions of coal pyrolysis by large-scale reactive molecular dynamics [J]. *J. Anal. Appl. Pyrolysis* **2021**, *155*, No. 105048.
(36) Hong, D.; Guo, X. Molecular dynamics simulations of Zhundong coal pyrolysis using reactive force field [J]. *Fuel* **2017**, *210*, 58−66.
(37) Chen, Y. F.; Tang, J.; Wang, Q. H.; Jia, X. Effect of gas residence time on pyrolysis products of fluidized bed lignite [J]. *J. Eng. Therm. Energy Power* **2017**, *32*, 62−67.
(38) Pather, T. S.; Al-Masry, W. A. The influence of bed depth on secondary reactions during slow pyrolysis of coal [J]. *J. Anal. Appl. Pyrolysis* **1996**, *37*, 83−94.
(39) He, X.; Zhu, H. Q.; Huo, Y. J.; Wang, W. *Study on the Formation Mechanism of the Pyrolysis Products of Lignite at Different Temperatures Based on ReaxFF-MD [J]*; America Chemical Society: ACS Omega, Washington, 2021; Vol. *6*, pp 35572−35583.
(40) Li, R. Z. Thermodynamic analysis of aromatic hydrocarbon generation during coal pyrolysis (I) [J]. *Iron Steel* **1954**, *02*, 70−75.
(41) Li, R. Z. Thermodynamic Analysis of Aromatic Hydrocarbon Formation during Coal Pyrolysis (II) [J]. *Iron Steel* **1954**, *03*, 58−60.
(42) Fu, X. C. *Physical Chemistry [M]*, 5th ed.; Higher Education Press, 2005.
(43) Maier Chas, G.; Kelley, K. K. An Equation For The Representation Of High-temperature Heat Content Data 1 [J]. *J. Am. Chem. Soc.* **1932**, *54*, 3243−3246.
(44) Denisova, L. T.; Belousova, N. V.; Galiakhmetova, N. A.; Denisov, V. M. Heat capacity of $GdBiGeO_5$ in the temperature range 373−1000 K [J]. *Dokl. Phys. Chem.* **2017**, *473*, 58−60.
(45) Denisova, L. T.; Irtyugo, L. A.; Kargin, Y. F.; Beletskii, V. V.; Denisov, V. M. Synthesis and high-temperature heat capacity of $Gd_2Sn_2O_7$ [J]. *Inorg. Mater.* **2016**, *52*, 584−586.
(46) Dou, Y. Y.; Zhong, W. Q.; Zhou, G. W.; Liu, Q.; Yin, J. P. Characteristics of tar and gas produced from coal Pressurized and low temperature pyrolysis [J]. *J. Southeast Univ.* **2018**, *48*, 85−91.
(47) Liao, H.; Li, B.; Zhang, B. Co-pyrolysis of coal with hydrogen-rich gases. 1. Coal pyrolysis under coke oven gas and synthesis gas [J]. *Fuel* **1998**, *77*, 847−851.
(48) Cyprès, R.; Furfari, S. Fixed-bed pyrolysis of coal under hydrogen pressure at low heating rates [J]. *Fuel* **1981**, *60*, 768−778.
(49) Cui, Y. P.; Qin, L. L.; Du, J. *Products Distribution and its Influencing Factors for Coal Pyrolysis [J]*; Coal Chemical Industry, 2007.

https://doi.org/10.1021/acsomega.2c08033
ACS Omega 2023, 8, 12805−12819